



## Polymeric Janus nanorods *via* anodic aluminum oxide templating†

 Xia Huang, \*<sup>abc</sup> Hatice Mutlu, <sup>d</sup> Wenyuan Dong<sup>bc</sup> and Patrick Theato \*<sup>bc</sup>

 Cite this: *Soft Matter*, 2023, 19, 5663

 Received 8th June 2023,  
Accepted 8th July 2023

DOI: 10.1039/d3sm00751k

rsc.li/soft-matter-journal

**We report a novel method for the fabrication of polymeric Janus nanorods *via* sequential polymerization from anodic aluminum oxide (AAO) templates. Dual compositions can be incorporated into individual nanorods and endow versatile potential applications. This fabrication strategy paves the way for constructing multifunctional nanostructures and brings together different materials in a single entity.**

Janus nanoparticles, named after a Roman god who has two opposite and distinct faces, are asymmetric nanoparticles that consist of distinct chemical or physical properties.<sup>1</sup> Indeed, the dual nature of Janus nanoparticles offers them diverse properties such as the capability to target complex self-assembled structures,<sup>2</sup> unique surface properties devoted as a stabilizer<sup>3</sup> or built-in multi-stimulus responsiveness,<sup>4</sup> which are inconceivable for homogenous particles. Multifunctional Janus nanoparticles show potential applications as solid surfactants,<sup>5</sup> drug cargos,<sup>6</sup> self-propelled nanomotors,<sup>7</sup> building blocks towards specific superstructures,<sup>2</sup> *etc.* Thus, plenty of Janus nanoobjects have been attained, from the simplest spherical structures to different heterotypes such as dumbbell-form, and disk-shaped or cylindrical-shaped structures. In fact, nanorods, nanotubes, and nanowires have high aspect ratios, which offers them superior applications to build two- or three-dimensional nanostructures.<sup>8</sup> For instance, Park *et al.* have fabricated a

dumbbell-shaped amphiphilic Janus nanoparticle designed for the construction of three-dimensional photonic crystals.<sup>9</sup> So far, many techniques have been used to fabricate Janus nanoparticles, such as Pickering emulsion polymerization, surface-initiated polymerization, fluidic nanoprecipitation and template methods.<sup>10,11</sup> In the midst of nanostructure fabrication methods, the template synthesis method is a cost-effective method for preparing one-dimensional nanostructures with high throughput.<sup>12</sup> Amongst them, the AAO template is one of the widely used templates applied for the preparation of nanoobjects.<sup>13</sup> Indeed, Choi's work illustrates the fabrication of asymmetric nanopillars.<sup>14</sup> Meanwhile, Hurst *et al.* reported that by means of AAO template synthesis, metal-polymer Janus nanorods were prepared, and attributed to the asymmetric nature, these nanorods had the ability to self-assemble into superstructures.<sup>8</sup> Although substantial research has been performed on the preparation of one-dimensional Janus nanoparticles, the majority of these works are focused on inorganic-inorganic or polymer-inorganic nanostructures. Interestingly, little research has been reported about the preparation of polymeric Janus nanoparticles *via* AAO templating. As a matter of fact, polymers are good candidates to replace metals that are utilized in the fabrication of Janus particles. In particular, due to the fact that polymeric materials have better processability, that may facilitate nanostructure fabrication.<sup>15</sup> In addition, polymeric materials may possess functional groups, which enable post-polymerization modification.<sup>16–18</sup> In this regard, the preparation of polymeric Janus nanorods *via* AAO templating is highly intriguing as it involves the integration of diverse components into a single structure. This integration allows for distinct functionalizations, leading to unique performance in various fields.<sup>19</sup> By sequentially infiltrating a polymer or monomer into the hexagonally well-ordered pores of AAO templates, designed nanostructures can be obtained. The infiltration can be accomplished by wetting with either melts or solutions.<sup>20</sup> Additionally, owing to the tunable pore dimensions of AAO templates, nanostructures differing in length and diameter are easy to achieve.

<sup>a</sup> Centre for Biomaterials in Surgical Reconstruction and Regeneration, Division of Surgery and Interventional Science, University College London (UCL), London, NW3 2PF, UK. E-mail: xia.huang@ucl.ac.uk

<sup>b</sup> Institute for Chemical Technology and Polymer Chemistry (ITCP), Karlsruhe Institute of Technology (KIT), Engesserstr. 18, D-76131, Karlsruhe, Germany. E-mail: patrick.theato@kit.edu

<sup>c</sup> Soft Matter Laboratory, Institute for Biological Interfaces (IBG 3), Karlsruhe Institute of Technology (KIT), Hermann-von-Helmholtz-Platz, D76344, Eggenstein-Leopoldshafen, Germany

<sup>d</sup> University Haute de Alsace (UHA), Institut de Science des Matériaux de Mulhouse (IS2M), UMR 7361 CNRS/UHA, 15 rue Jean Starcky, 68057 Mulhouse Cedex, France

† Electronic supplementary information (ESI) available. See DOI: <https://doi.org/10.1039/d3sm00751k>



On account of this, a generally applicable strategy for the fabrication of polymeric Janus nanorods was developed by sequential polymerization of alternative chemical components in AAO templates. For instance, amphiphilic polystyrene-*block*-poly(*N*-*iso*-propylacrylamide) (PS-*b*-PNIPAm) Janus nanorods were first fabricated. The 'block' here represents the binding effect of the two components in each nanorod. Since the two blocks are chemically bonded, Janus nanorods can maintain their shape after dissolving out from the templates and with further design, this strategy is also applicable for preparing triple or multi-component nanorods.

Accordingly, we proposed a simple and efficient route for fabricating polymeric Janus nanorods bearing a poly(*N*-*iso*-propylacrylamide) (PNIPAm) block and a polystyrene (PS) block. Styrene monomer is selected owing to its easy accessibility and highly efficient polymerization behaviour, while PNIPAm *versus* PS blocks are distinguishable *via* transmission electron microscopy (TEM). By using low cost AAO as the template, uniform nanorods can be prepared with a high throughput. Following the process illustrated in Scheme 1, the PS nanorods were first formed *via* free-radical polymerization. In detail, a stock solution that consisted of styrene monomer, a crosslinker, a photo-crosslinker (*i.e.* 4-acryloylbenzophenone) and a thermal initiator (*i.e.* 2,2'-azobis(*iso*-butyronitrile), AIBN) was dissolved in anhydrous 1,4-dioxane. Accordingly, by drop casting the stock solution onto an AAO template, followed by thermally initiated polymerization, full-sized PS polymer blocks were formed inside of the AAO template (see ESI† Section C for more details on the fabrication of Janus PS-*b*-PNIPAm nanorods).

Subsequently, oxygen plasma treatment was conducted to eliminate the excess PS nanorods and crucially to generate sufficient space for the second polymer block. Thereafter, PNIPAm nanorods were formed in the AAO template on the top of each PS nanorod by adopting the aforementioned conditions. Ultimately, post-crosslinking was induced under UV treatment in and between the PS and PNIPAm nanorods; thus, Janus nanorods were collected after dissolving from AAO. With the introduction of 4-acryloylbenzophenone, the formed two blocks are chemically connected into a single Janus nanorod. Importantly, the two blocks could be replaced by using

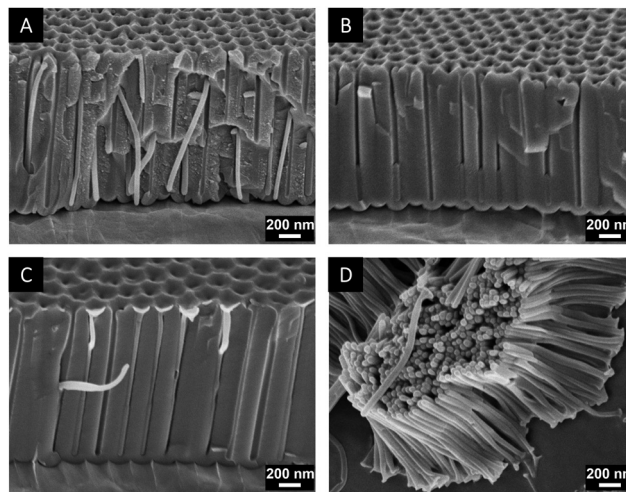


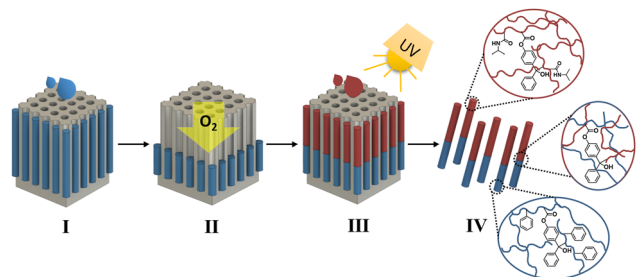
Fig. 1 SEM images of (A) PS nanorod-filled AAO template, (B) half-filled PS nanorods in the AAO template, (C) PS-*b*-PNIPAm Janus nanorods in the AAO template, and (D) bundles of crosslinked PS-*b*-PNIPAm Janus nanorods.

different monomers, thus building various functionalized Janus nanorods.

In order to monitor the transformation of morphologies during the fabrication process, SEM images of nanostructure samples were recorded at each step. From Fig. 1A, it can be seen that nanorod structures were formed, which filled completely the nanocavities of the AAO template, thus indicating the successful fabrication of PS nanorods *via in situ* free-radical polymerization. As previously mentioned, further oxygen plasma treatment was carried out to partially remove the formed PS nanorods. During oxygen plasma treatment, the generated oxygen plasma is inducing polymer etching and leading to the disappearance of the PS nanorods. By adjusting the treatment time to 30 min, approximately 1  $\mu\text{m}$  of PS block was removed as recorded in the SEM image shown in Fig. 1B.

Afterwards, a second free-radical polymerization was carried out in the template, resulting in the formation of a PNIPAm block inside of the membrane nanocavities above the pre-formed PS block. UV irradiation was then applied; thus, benzophenone units present in both PS and PNIPAm blocks led to crosslinking between the PS block and PNIPAm block.<sup>21</sup> Fig. 1C illustrates the SEM image of PS-*b*-PNIPAm Janus nanorods within the AAO template. A small junction between the PS block and PNIPAm block could be observed. After dissolving the AAO templates in 10 wt% aqueous  $\text{H}_3\text{PO}_4$ , the nanorods were filtered and washed thoroughly with distilled water, and the image of the collected Janus nanorods is recorded in Fig. 1D. As revealed, bundles of Janus nanorods were observed and all samples maintained distinct junctions, which demonstrated the successful fabrication of PS-*b*-PNIPAm Janus nanorods. In order to further depict the composition of the Janus nanorods, TEM observations as well as energy-dispersive X-ray (EDX) analysis were carried out and the results are recorded in Table 1.

As illustrated, the top part of the PS-*b*-PNIPAm Janus nanorod contained the highest amount of nitrogen atoms

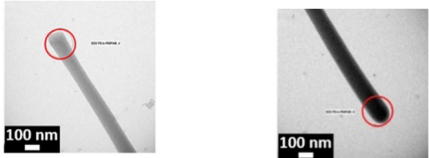


Scheme 1 Proposed route for the fabrication of PS-*b*-PNIPAm Janus nanorods. (I) *In situ* polymerization of the first PS block; (II) oxygen plasma treatment; (III) *in situ* polymerization of the second PNIPAm block and post-UV-crosslinking; and (IV) dissolution of the AAO template and release of PS-*b*-PNIPAm Janus nanorods.



**Table 1** Comparison of elemental components and TEM images of top and bottom points for the PS-*b*-PNIPAm Janus nanorods

Element	Top		Bottom	
	Weight%	Atomic%	Weight%	Atomic%
N	66.7	69.7	27.0	29.7
O	32.7	30.0	72.7	70.2
P	0.6	0.3	0.3	0.1

along the Janus nanorod. This phenomenon is in accordance with the fact that the top block of the Janus nanorod consisted of PNIPAm, which contained nitrogen atoms in the polymer chains. However, a smaller amount of nitrogen can also be found in the bottom of the nanorods. This could be attributed to the nitrogen atmosphere in the TEM sample chamber or the nitrogen resulting from the initiator.

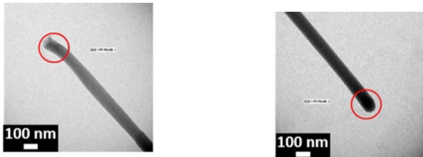
Additionally, it could be distinguished from the TEM images that the PS block is represented darker than the PNIPAm block, owing to the differences in the electron density between the PS and PNIPAm blocks.<sup>22</sup> As a consequence, the formation of Janus nanorods has been successfully demonstrated.

Additionally, the fabrication method is capable of preparing diverse Janus nanorods using various monomer species. Indeed, *via* adopting the same strategy, poly(*N*-isopropylacrylamide)-*b*-poly(pentafluorophenyl acrylate) (PNIPAm-*b*-PPFPA) nanorods were then prepared (ESI† Section D). The obtained Janus nanorods were also characterized by SEM to record their morphology and the results are illustrated in Fig. 2.

Furthermore, in order to prove the strict composition of the PNIPAm-*b*-PPFPA nanorods, compositional TEM and EDX analyses of PNIPAm-*b*-PPFPA Janus nanorods were carried out. The obtained results are illustrated in Table 2. Obviously, the content of nitrogen in the top block is much less than that in the bottom block, which is in accordance with the composition of each block; in other words, the bottom PNIPAm block contains nitrogen while the top PPFPA block does not. However, residual small amounts of nitrogen may again be attributed to the atmosphere of the sample chamber or remains of the thermal initiator. On the contrary, fluorine was found at 21.2 wt% in the top PPFPA block, while only traces of fluorine

**Table 2** Comparison of elemental components and TEM images of top and bottom points for the PNIPAm-*b*-PPFPA Janus nanorods

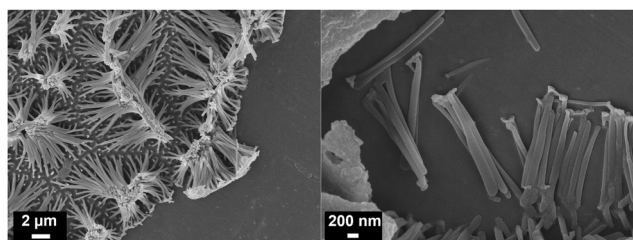
Element	Top		Bottom	
	Weight%	Atomic%	Weight%	Atomic%
N	57.0	60.5	11.6	13.5
O	41.5	38.5	66.7	68.0
F	0.9	0.7	21.2	18.2
Al	0.2	0.1	0.1	0.1
P	0.2	0.1	0.2	0.1
S	0.3	0.1	0.2	0.1

element content were found in the PNIPAm block, which confirmed the composition of each block in the Janus PNIPAm-*b*-PPFPA nanorods. In addition, electron density differences as well as the junction between the two blocks are clearly distinguished in the TEM images, ultimately proving that the PNIPAm-*b*-PPFPA Janus nanorods were obtained.

As mentioned above, Janus nanorods bearing different chemical composition are easy to fabricate *via* the AAO templating strategy. In order to prepare Janus nanorods that not only differ in chemical composition but also in shape morphology, complex Janus nanorods that are composed of a polypyrrole nanoparticle (PPyNP) block and poly(methyl methacrylate) (PMMA) block are fabricated (ESI† Section E). The detailed fabrication process is illustrated in Scheme 2.

In detail, the as-prepared AAO membrane was first immersed in an aqueous solution that consisted of NaOAc, FeCl<sub>3</sub> and pyrrole. Subsequently, the mixture was sonicated for 0.5 h at room temperature. During sonication, pyrrole was polymerized under oxidation of FeCl<sub>3</sub> and the formation of PPyNP was observed, which in turn spread on the template surface and in the membrane pores, respectively. Upon rinsing, SEM analysis of the AAO template was performed, the resulting SEM images using an inserted optical image are illustrated in Fig. 3. It could be observed that, after sonication, PPyNPs are formed and distributed homogeneously on the AAO surface as well as inside of the membrane channels. Subsequently, the PPyNP-filled template was exposed to oxygen plasma to remove the redundant PPyNPs and leave space for the second block. A PMMA block was then

**Fig. 2** SEM images of PNIPAm-*b*-PPFPA Janus nanorods.**Scheme 2** Schematic illustration of preparing PPyNP-*b*-PMMA Janus nanorods. (I) *In situ* polymerization of PPyNP nanoparticles; (II) oxygen plasma treatment; (III) *in situ* polymerization of the PMMA block; and (IV) dissolution of the AAO template and release of PPyNP-*b*-PMMA Janus nanorods.

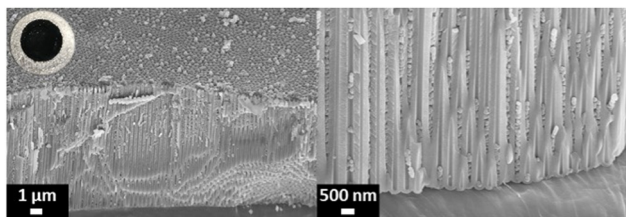


Fig. 3 Optical image and scanning electron micrographs of PPyNP in the AAO template.

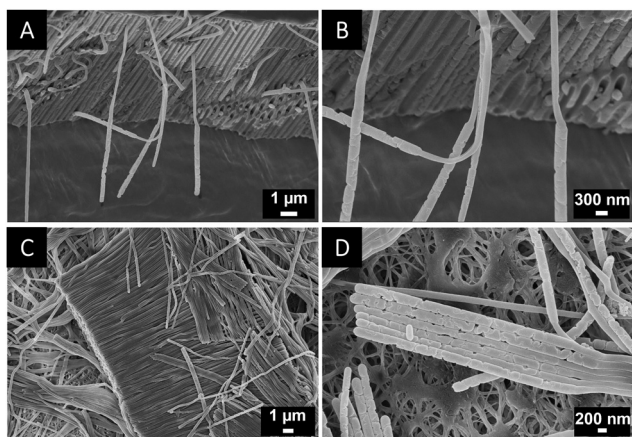


Fig. 4 Scanning electron micrographs of PPyNP-*b*-PMMA Janus nanorods (A) and (B) in the AAO template and (C) and (D) freely dispersed.

synthesized under confinement in the AAO template and dispersed Janus nanorods were obtained after dissolving the AAO.

SEM images of polypyrrole nanoparticle-*b*-poly(methyl methacrylate) (PPyNP-*b*-PMMA) Janus nanorods were recorded, as shown in Fig. 4. It can be clearly seen from Fig. 4 that the Janus nanorods are composed of two distinct parts, as expected; the rough block is a stack of PPyNP nanoparticles, while the smooth block consists of PMMA.

Moreover, in order to further visualize the compositional structure of PPyNP-*b*-PMMA Janus nanorods, TEM was carried out and is shown in Fig. 5. From the TEM image, two distinguishable blocks could be observed in each individual nanorod, which confirmed the successful fabrication. The formed Janus nanorods not only differ in chemical composition, but also reveal different morphologies in each block.

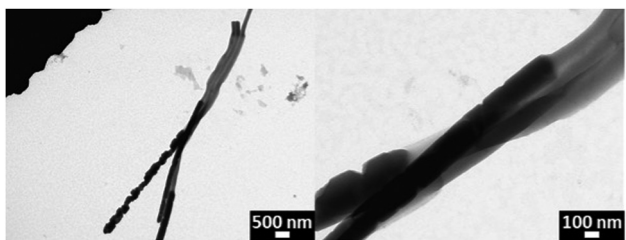


Fig. 5 Transmission electron micrographs of PPyNP-*b*-PMMA Janus nanorods.

To conclude, two types of polymeric Janus nanorods have been successfully fabricated *via* AAO templating. The PS-*b*-PNIPAm and PNIPAm-*b*-PPFPA nanorods differed in chemical composition. Besides, PPyNP-*b*-PMMA nanorods that depict differences in composition and shape are also achievable. Additionally, due to the specific optical performance of PPyNP, this kind of Janus nanorod has the potential to be used as a self-propelled nanomotor. The results demonstrate that various kinds of Janus nanorods, which differ in chemical composition or/and shape, can be produced by employing a simple template-based strategy. Clearly, benefits of the approach presented here are not limited to the materials mentioned above, thereby opening up plenty of new possibilities for fabricating complex nanostructures with potential applications in surfactants, and as building blocks for self-assembling or constructing optical devices amongst others.

## Author contributions

X. H. conceptualization, methodology, investigation, and visualization. W. D. conceptualization, methodology. H. M. methodology, writing – review and editing, and supervision. P. T. funding acquisition, conceptualization, supervision, visualization, and writing – review and editing. H. M. and P. T. conceived and supervised this work. X. H. performed the fabrication, characterization of Janus nanorods and wrote the manuscript. W. D. designed the figures.

## Conflicts of interest

There are no conflicts to declare.

## Acknowledgements

X. H. and W. D. gratefully acknowledge the China Scholarship Council (CSC grant: 201506240019 and 201707565012) for partial support of this work. H. M. acknowledges the University of Haute-Alsace for financial support from the French National Research Agency with the reference “ANR-22-CPJ1-0077-01” and from the CNRS for a junior professorship contract.

## References

- 1 M. Lattuada and T. A. Hatton, *Nano Today*, 2011, **6**, 286–308.
- 2 S. C. Glotzer and M. J. Solomon, *Nat. Mater.*, 2007, **6**, 557–562.
- 3 B. T. T. Pham, C. H. Such and B. S. Hawkett, *Polym. Chem.*, 2015, **6**, 426–435.
- 4 X. Liu, Y. Yang and M. W. Urban, *Macromol. Rapid Commun.*, 2017, **38**, 1–20.
- 5 F. Tu and D. Lee, *J. Am. Chem. Soc.*, 2014, **136**, 9999–10006.
- 6 H. Xie, Z. G. She, S. Wang, G. Sharma and J. W. Smith, *Langmuir*, 2012, **28**, 4459–4463.
- 7 X. Ma, K. Hahn and S. Sanchez, *J. Am. Chem. Soc.*, 2015, **137**, 4976–4979.



- 8 S. J. Hurst, E. K. Payne, L. Qin and C. A. Mirkin, *Angew. Chem., Int. Ed.*, 2006, **45**, 2672–2692.
- 9 J. Park, J. D. Forster and E. R. Dufresne, *J. Am. Chem. Soc.*, 2010, **132**, 5960–5961.
- 10 N. Haberkorn, K. Nilles, P. Schattling and P. Theato, *Polym. Chem.*, 2011, **2**, 645–650.
- 11 J. Du and R. K. O'Reilly, *Chem. Soc. Rev.*, 2011, **40**, 2402–2416.
- 12 H. Jo, N. Haberkorn, J.-A. Pan, M. Vakili, K. Nielsch and P. Theato, *Langmuir*, 2016, **32**, 6437–6444.
- 13 X. Huang, H. Mutlu and P. Théato, *Colloid Polym. Sci.*, 2021, **299**, 325–341.
- 14 M. K. Choi, H. Yoon, K. Lee and K. Shin, *Langmuir*, 2011, **27**, 2132–2137.
- 15 J. W. Hickey, J. L. Santos, J.-M. Williford and H.-Q. Mao, *J. Controlled Release*, 2015, **219**, 536–547.
- 16 N. S. Enikolopyan, M. L. Fridman, I. O. Stalnova and V. L. Popov, *Filled Polymers: Science and Technology*, Springer, 1990, pp. 1–67.
- 17 J. Ruiz, B. Gonzalo, J. R. Dios, J. M. Laza, J. L. Vilas and L. M. León, *Adv. Polym. Technol.*, 2013, **32**, 180–188.
- 18 E. L. Kalinchev, *Int. Polym. Sci. Technol.*, 2002, **29**, 55–62.
- 19 X. Zhang, Q. Fu, H. Duan, J. Song and H. Yang, *ACS Nano*, 2021, **15**, 6147–6191.
- 20 X. She, G. Song, J. Li, P. Han, S. Yang, W. Shulong and Z. Peng, *Polym. J.*, 2006, **38**, 639–642.
- 21 G. Stoychev, N. Puretskiy and L. Ionov, *Soft Matter*, 2011, **7**, 3277–3279.
- 22 J. Kikuchi and K. Yasuhara, *Transmission electron microscopy. Supramolecular chemistry: From molecules to nanomaterials*, John Wiley & Sons, Ltd, 2012.

